

Magneto–Structural Correlations in 2D and 3D Extended Structures of Manganese(II)–Malonate Systems

Tapas Kumar Maji,[†] Saugata Sain,[†] Golam Mostafa,[‡] Tian-Huey Lu,[‡] Joan Ribas,^{*,§} Montserrat Monfort,[§] and Nirmalendu Ray Chaudhuri^{*,†}

[†]Department of Inorganic Chemistry, Indian Association for the Cultivation of Science, Kolkata-700 032, India, [‡]Department of Physics, National Tsing-Hua University, Hsinchu 300, ROC, and [§]Departament de Química Inorgànica, Universitat de Barcelona, Diagonal, 647, 08028-Barcelona, Spain

Received March 28, 2002

Two polymeric malonato-bridged manganese(II) complexes of formula $[\text{Mn}(\text{mal})(\text{H}_2\text{O})_2]_n$ (**1**) and $[\text{Mn}_2(\text{mal})_2(4,4'\text{-bipy})(\text{H}_2\text{O})_2]_n$ (**2**) have been synthesized and characterized (mal = malonate dianion; 4,4'-bipy = 4,4'-bipyridine). The crystal structure of complex **1** was already known. Complex **2** crystallizes in monoclinic space group $P2_1/n$, $Z = 2$, with unit cell parameters of $a = 7.2974(10)$ Å, $b = 18.7715(10)$ Å, $c = 7.514(3)$ Å, and $\beta = 91.743(12)^\circ$. The structure determination reveals that the complex $[\text{Mn}_2(\text{mal})_2(4,4'\text{-bipy})(\text{H}_2\text{O})_2]_n$ (**2**) is a 3D network being composed of Mn–malonate sheets which are pillared by bidentate 4,4'-bipy spacer forming small voids. The Mn–Mn distances through Mn– μ -(O3–C8–O4)–Mn, Mn– μ -(O1–C6–O2)–Mn, and Mn– μ -4,4'-bipy–Mn bridges are 5.561, 5.410, and 11.723 Å, respectively. The magnetic behaviors of complexes **1** and **2** in the temperature range 300–2 K are very close, corresponding to a weak antiferromagnetic coupling. The magnetic pathways of complex **1** are through two Mn–O–C–O–Mn with *anti-anti* conformation and two Mn–O–C–O–Mn with *syn-anti* conformations and in complex **2** through all Mn–O–C–O–Mn with *syn-anti* conformations. Both *syn-anti* and *anti-anti* conformations create weak antiferromagnetic coupling, and the susceptibility data are fitted by the expansion series of Lines and the Curély formula for an $S = 5/2$ antiferromagnetic quadratic layer, based on the exchange Hamiltonian $H = -\sum_{nr} JS_i S_j$. The best fit is given by the superexchange parameters $J = -0.32$ cm⁻¹ and $g = 2.00$ for complex **1** and $J = -0.14$ cm⁻¹, $J_{\text{inter}} = -0.031$ cm⁻¹, and $g = 2.00$ for complex **2**. Finally, in both the complexes there is a magnetic pathway Mn–O–C–C–O–Mn, and this pathway through the three carbon atoms of the malonato-bridging ligand could be considered negligible.

Introduction

Investigation of novel inorganic–organic hybrid framework assemblies represents one of the most active areas of material science and chemical research.¹ The intense interest in these materials is driven to a large extent by their

interesting properties and potential in various applications, e.g., electrical conductivity, magnetism, host–guest chemistry, ion exchange, catalysis, nonlinear optics, etc.² Therefore, rational design and construction of new materials with specific networks has become a particularly important and topical subject. The key to the construction of a desired framework with specific dimensionality (1D/2D/3D) is the selection of suitable organic building block.

Recently the use of organic spacers, particularly the dicarboxylic acids as superexchange pathways between the

* To whom correspondence should be addressed. E-mail: icnrc@mahendra.iacs.res.in (N.R.C.). Fax: 91-33-2473 2805.

[†] Indian Association for the Cultivation of Science.

[‡] National Tsing-Hua University.

[§] Universitat de Barcelona.

(1) (a) *Inorganic Materials*; Bruce, D. W., O'Hare, D., Eds.; John Wiley & Sons: New York, 1992. (b) *Magneto Structural Correlations in Exchange Coupled Systems*; Willet, R. D., Gatteschi, D., Kahn, O., Eds.; NATO ATI Series C140; Reidel: Dordrecht, The Netherlands, 1985. (c) Moulton, B.; Zaworotko, M. J. *Chem. Rev.* **2001**, *101*, 1629. (d) Hagrman, P. J.; Hagrman, D.; Zubietta, J. *Angew. Chem., Int. Ed.* **1999**, *38*, 2638. (e) Robson, R. *J. Chem. Soc., Dalton Trans.* **2000**, 3735.

(2) (a) Su, W.; Hong, M.; Weng, J.; Cao, R.; Lu, S. *Angew. Chem., Int. Ed.* **2000**, *39*, 2911. (b) *Molecular Magnetic Materials*; Gatteschi, D., Kahn, O., Miller, J., Eds.; Nato ASI Series E198; Kluwer: Dordrecht, The Netherlands, 1991. (c) Yaghi, O. M.; Li, G.; Li, H. *Nature* **1995**, *378*, 703. (d) Marouka, K.; Murase, N.; Yamamoto, H. *J. Org. Chem.* **1993**, *58*, 2938. (e) Chen, C.; Suslick, K. S. *Coord. Chem. Rev.* **1993**, *128*, 293 and references therein.

metal ions [Cu(II), Mn(II), Ni(II), etc.], is of growing interest in the field of molecular magnetism³ as well as there is an increased recognition of the metals' role in biological systems.⁴ Carboxylato-bridged manganese(II) complexes are of special interest, since such systems are known to exist at the active centers of some manganese-containing enzymes.⁵ Among the dicarboxylates, the major studies have been done on oxalate and terephthalate^{6–8} and a few examples with malonate, fumarate, maleate, adipate, etc.^{9–20} Among them, malonate dianion functions as a versatile bridging ligand and the structural complexity in its metal complexes is associated with the simultaneous adoption of chelating bidentate and different carboxylato-bridging coordination modes (*syn-syn*, *anti-anti*, and *syn-anti*).^{9–14} The magneto–structural correlation indicates that the malonato-bridging ligand has the ability to mediate simultaneously weak but significant antiferromagnetic interaction through the carboxylato bridge in *syn-anti* conformation and antiferromagnetic through the OCCCO skeleton in *anti-anti* conformations. These observations agree very well with that reported very recently by Ruiz-Pérez et al. in other (malonato)copper(II) derivatives.^{10,11} But to the best of our knowledge the magneto–

structural correlation in the (malonato)manganese(II) system has yet to be reported.

In this work, we report the synthesis, structural characterization, and magnetic investigation of two complexes of formulas $[\text{Mn}(\text{mal})(\text{H}_2\text{O})_2]_n$ (**1**) (crystal structure already reported) and $[\text{Mn}_2(\text{mal})_2(4,4'\text{-bipy})(\text{H}_2\text{O})_2]_n$ (**2**). These two complexes illustrate both the versatility of malonate as ligand toward manganese(II) and the importance of structural knowledge in magnetic studies. The low-temperature magnetic measurement reveals that both the complexes show weak antiferromagnetic interaction through the *syn-anti* and *anti-anti* bridging modes.

Experimental Section

Materials. Manganese(II) chloride tetrahydrate and 4,4'-bipyridine were purchased from Aldrich Chemical Co. Inc., and the other chemicals used were of AR grade.

Synthesis of Complex $[\text{Mn}(\text{mal})(\text{H}_2\text{O})_2]_n$ (1**).** Manganese(II) chloride tetrahydrate (0.197 g, 1 mmol) dissolved in 10 mL of methanol was allowed to react with a 5 mL of an aqueous solution of disodium malonate (0.148 g, 1 mmol) in a round-bottom flask. The entire reaction mixture was refluxed for 24 h, cooled, and filtered. The filtrate was allowed to evaporate slowly in a vacuum desiccator. After 2 weeks needle-shaped single crystals suitable for X-ray structure determination were obtained. These were filtered off, washed thoroughly with 2-propanol, and dried. Yield: 75%. Anal. Calcd for $\text{C}_3\text{H}_{10}\text{O}_8\text{Mn}$ (**1**): C, 15.7; H, 4.4; Mn, 24.0. Found: C, 15.7; H, 4.3; Mn, 23.9.

Synthesis of Complex $[\text{Mn}_2(\text{mal})_2(4,4'\text{-bipy})(\text{H}_2\text{O})_2]_n$ (2**).** Manganese(II) chloride tetrahydrate (0.197 g, 1 mmol) dissolved in 10 mL of methanol was allowed to react with 5 mL of an aqueous solution of disodium malonate (0.148 g, 1 mmol) and stirred for 20 min. Into the resulting solution was poured slowly 5 mL of a methanolic solution of 4,4'-bipyridine (0.156 g, 1 mmol), the entire mixture was stirred for 2 h and filtered, and the pale yellow filtrate was allowed to evaporate slowly in an open atmosphere. After a few days pale yellow diamond-shaped single crystals suitable for X-ray structural study were obtained. These were separated, washed with 2-propanol, and dried. Yield: 80%. Anal. Calcd for $\text{C}_{13}\text{H}_{12}\text{N}_2\text{O}_5\text{Mn}_2$ (**2**): C, 47.1; H, 3.6; N, 8.5; Mn, 16.6. Found: C, 47.1; H, 3.7; N, 8.6; Mn, 16.5.

Physical Measurements. Elemental analyses (C, H, N) were carried out using a Perkin-Elmer 240C elemental analyzer. The IR spectra were recorded (4000–400 cm^{-1}) on a Nicolet 520 FTIR spectrometer as KBr pellets. The thermal analysis (TGA) was carried out using a Shimadzu DT-30 thermal analyzer under a flow of dinitrogen (30 mL min^{-1}). The sample (particle size 50–200 mesh) was heated at a rate of 10 $^\circ\text{C min}^{-1}$ with inert alumina as a reference. Magnetic measurements were carried out on polycrystalline samples (30–40 mg) with a Quantum Design MPMS SQUID susceptometer operating at a magnetic field of 0.1 T between 2 and 300 K. The diamagnetic corrections were evaluated from Pascal's constants. EPR spectra were recorded on powder samples at X-band frequency with a Bruker 300E automatic spectrometer, varying the temperature between 4 and 300 K.

Crystallographic Data Collection and Refinement. A suitable single crystal of complex **2** was mounted on a Enraf-Nonius CAD4 single-crystal diffractometer. The unit cell parameters and crystal orientation matrix were determined by least-squares refinements of 25 accurately centered reflections. Intensity data were collected in the ω - 2θ scan mode using graphite-monochromated $\text{Mo K}\alpha$

- (3) (a) Oldham, C. In *Comprehensive Coordination Chemistry*; Wilkinson, G., Gillard, R. D., McCleverty, J. A., Eds.; Pergamon Press: Oxford, U.K., 1987; Vol. 2, p 435. (b) Kahn, O. *Molecular Magnetism*; VCH: New York, 1993.
- (4) (a) Christou, G. *Acc. Chem. Res.* **1989**, *22*, 328. (b) Wiegardt, K. *Angew. Chem., Int. Ed. Engl.* **1989**, *28*, 1153.
- (5) (a) *Manganese Redox Enzymes*; Pecoraro, V. L., Ed.; VCH: New York, 1992. (b) Waldo, G. S.; Yu, S.; Penner-Hahn, J. E. *J. Am. Chem. Soc.* **1992**, *114*, 5869. (c) Tan, X. S.; Xiang, D. F.; Tang, W. X.; Sun, J. *Polyhedron* **1997**, *16*, 689. (d) Policar, C.; Lambert, F.; Cesario, M.; Morgenstern-Badarau, I. *Eur. J. Inorg. Chem.* **1999**, 2201 and references therein. (e) Tangoulis, V.; Psomas, G.; Dendrinou-Samara, C.; Raptopoulou, C. P.; Terzis, A.; Kessissoglou, D. P. *Inorg. Chem.* **1996**, *35*, 7655. (f) Albela, B.; Corbella, M.; Ribas, J.; Castro, I.; Sletten, J.; Stoeckli-Evans, H. *Inorg. Chem.* **1998**, *37*, 788. (g) Xen, X. M.; Tong, Y. X.; Xu, Z. T.; Mak, T. C. W. *J. Chem. Soc., Dalton Trans.* **1995**, 4001.
- (6) Girerd, J. J.; Kahn, O.; Verdager, M. *Inorg. Chem.* **1980**, *19*, 274.
- (7) (a) Julve, M.; Verdager, M.; Gleizes, A.; Philoche-Lavalisles, M.; Kahn, O. *Inorg. Chem.* **1984**, *23*, 3808. (b) Julve, M.; Faus, J.; Verdager, M.; Gleizes, A. *J. Am. Chem. Soc.* **1984**, *106*, 3808.
- (8) (a) Deakin, L.; Ariff, A. M.; Miller, J. S. *Inorg. Chem.* **1999**, *38*, 5072 and references therein. (b) Lo, M.-F. S.; Chui, S.-Y. S.; Shek, L. Y.; Lin, Z.; Zhang, X. X.; Wen, G. H.; Williams I. D. *J. Am. Chem. Soc.* **2000**, *122*, 6293.
- (9) Li, J.; Zeng, H.; Chen, J.; Wang, Q.; Wu, X. *Chem. Commun.* **1997**, 1213.
- (10) Ruiz-Pérez, C.; Hernández-Molina, M.; Lorenzo-Luis, P.; Lloret, F.; Cano, J.; Julve, M. *Inorg. Chem.* **2000**, *39*, 3845.
- (11) Ruiz-Pérez, C.; Sanchiz, J.; Hernández-Molina, M.; Lloret, F.; Julve, M. *Inorg. Chem.* **2000**, *39*, 1363 and references therein.
- (12) Lightfoot, P.; Snedden, A. *J. Chem. Soc., Dalton Trans.* **1999**, 3549.
- (13) Lis, T.; Matuszewski, J. *Acta Crystallogr.* **1979**, *35B*, 2212.
- (14) Muro, G. D.; Mautner, F. A.; Insausti, M.; Lezema, L.; Arriortua, M. I.; Rojo, T. *Inorg. Chem.* **1998**, *37*, 3243.
- (15) (a) Mukherjee, P. S.; Dalai, S.; Mostafa, G.; Zangrando, E.; Lu, T. H.; Rogez, G.; Mallah, T.; Ray Chaudhuri, N. *Chem. Commun.* **2001**, 1346. (b) Dalai, S.; Mukherjee, P. S.; Zangrando, E.; Lloret, F.; Ray Chaudhuri, N. *J. Chem. Soc., Dalton Trans.* **2002**, 822.
- (16) Mukherjee, P. S.; Maji, T. K.; Mostafa, G.; Ribas, J.; Salah El Fallah, M.; Ray Chaudhuri, N. *Inorg. Chem.* **2001**, *40*, 928.
- (17) Konar, S.; Mukherjee, P. S.; Zangrando, E.; Lloret, F.; Ray Chaudhuri, N. *Angew. Chem., Int. Ed.* **2002**, *41*, 1561.
- (18) Shi, Z.; Zhang, L.; Gao, S.; Yang, G.; Jia, H.; Gao, L.; Feng, S. *Inorg. Chem.* **2000**, *39*, 1990.
- (19) Alyea, E. C.; Dias, S. A.; Ferguson, G.; Khan, M. A.; Roberts, P. J. *Inorg. Chem.* **1979**, *18*, 2433.
- (20) Kim, Y.; Jung, D. K. *Inorg. Chem.* **2000**, *39*, 1470 and references therein.

Table 1. Crystal Data and Details of the Structure Determination for Complex **2**

chem formula	C ₁₆ H ₁₆ Mn ₂ N ₂ O ₁₀
fw	506.18
temp (K)	297(2) K
wavelength	0.710 73 Å
cryst system	monoclinic
space group	<i>P</i> 2 ₁ / <i>n</i>
<i>a</i> (Å)	7.2974(10)
<i>b</i> (Å)	18.7715(10)
<i>c</i> (Å)	7.514(3)
β (deg)	91.743(12)
<i>V</i> (Å ³)	1028.8(4)
<i>Z</i>	2
ρ_{calc} (g/cm ³)	1.634
μ (mm ⁻¹)	1.283
<i>F</i> (000)	512
cryst size (mm)	0.27 × 0.19 × 0.17
θ range (deg)	2.91–26.99
reflens colld	4589
indpdt reflens	2083 [R(int) = 0.0167]
reflens obsd [<i>I</i> > 2 σ (<i>I</i>)]	1729
R indices [<i>I</i> > 2 σ (<i>I</i>)]	R1 = 0.0428, wR2 = 0.1393
R indices (all data)	R1 = 0.0520, wR2 = 0.1431

radiation ($\lambda = 0.710\ 73\ \text{\AA}$). The crystal and instrument stabilities were monitored with a set of 3 standard reflections measured at a regular interval; in all cases no significant variations were found. The intensity data were corrected for Lorentz and polarization effects,²¹ and an empirical absorption correction based on Ψ scans was also employed. A total of 4589 reflections were measured, and 2083 reflections were unique ($R_{\text{int}} = 0.017$). The structure was solved by Patterson synthesis and followed by successive Fourier and difference Fourier syntheses. Full-matrix least-squares refinements on F^2 were carried out using SHELXL-97 with anisotropic displacement parameters for all non-hydrogen atoms. Hydrogen atoms of water molecules were located from difference Fourier and refined isotropically. At convergence, the final residuals were $R1 = 0.0428$ and $wR2 = 0.1393$ for 1729 reflection with $I > 2\sigma(I)$. The final differences Fourier map showed the maximum and minimum peak heights at 1.32 and $-0.49\ \text{e}\text{\AA}^{-3}$, respectively, having no chemical significance. Complex neutral atom scattering factors²² were used throughout. All calculations were carried out using SHELXS-97,²³ SHELXL-97,²⁴ PLATON 99,²⁵ and ORTEP-3²⁶ programs. Crystallographic data and selected bond lengths and angles are given in Tables 1 and 2, respectively. H-bonding parameters are displayed in Table 3.

Results and Discussion

IR Spectroscopy. The IR spectra of both compounds **1** and **2** show broad bands in the region 3300–3500 cm^{-1} , which can be assigned to the stretching vibrations, $\nu(\text{O}–\text{H})$, of the hydroxyl group in the water molecules. The next group of bands appears at around 2800–2900 cm^{-1} and corresponds to the stretching vibrations, $\nu(\text{C}–\text{H})$, of the

Table 2. Selected Bond Lengths (Å) and Angles (deg) for Complex **2**

Mn–O2	2.115(2)	Mn–O3	2.216(3)
Mn–O1	2.124(2)	Mn–O5w	2.236(3)
Mn–O4	2.214(2)	Mn–N1	2.290(3)
O2–Mn–O1	171.9(1)	O4–Mn–O5w	90.9(1)
O2–Mn–O4	101.3(1)	O3–Mn–O5w	91.31(1)
O1–Mn–O4	86.7(1)	O2–Mn–N1	84.70(1)
O2–Mn–O3	88.9(1)	O1–Mn–N1	94.24(1)
O1–Mn–O3	83.0(1)	O4–Mn–N1	93.73(1)
O4–Mn–O3	169.5(1)	O3–Mn–N1	84.89(1)
O2–Mn–O5w	90.1(1)	O5w–Mn–N1	173.58(1)
O1–Mn–O5w	90.4(1)		

Table 3. Hydrogen Bonds (Å, deg) for Complex **2**

D–H ^a	<i>d</i> (D–H)	<i>d</i> (H \cdots A)	<i>d</i> (D \cdots A)	\angle DHA
O5W–H1W \cdots O1 ⁱ	0.91(6)	1.82(6)	2.673(4)	156(5)
O5W–H2W \cdots O3 ⁱⁱ	0.95(7)	1.81(7)	2.745(4)	166(5)

Symmetry code: (i) $1/2 + x, 1/2 - y, 1/2 + z$; (ii) $1/2 + x, 1/2 - y, -1/2 + z$.

malonate ligand.²⁷ The uncoordinated malonate shows a strong $\nu_{\text{as}}(\text{OCO})$ band at 1700 cm^{-1} and $\nu_{\text{s}}(\text{OCO})$ band at 1400 cm^{-1} . It also shows two medium-intensity bands at 800 and 750 cm^{-1} assigned to the OCO bending frequencies. These frequencies are significantly shifted to lower frequencies in both complexes on coordination to manganese(II) ions. In complex **1** $\nu_{\text{as}}(\text{OCO})$ and $\nu_{\text{s}}(\text{OCO})$ appear at $\sim 1570\ \text{cm}^{-1}$ and $\sim 1383\ \text{cm}^{-1}$, respectively, and for complex **2** at ~ 603 and $1390\ \text{cm}^{-1}$, which is significantly lower and indicative of the coordination of all the carboxylate to manganese(II) centers.^{10,11,14} Finally the bending vibration corresponding to the $\delta(\text{C}=\text{O})$ group is observed in the 1180–1300 cm^{-1} range for both compounds.

Crystal Structure of Complex 1. We have redetermined the crystal structure of complex **1** and found all the parameters are same with the results reported by Matuszewski et al.¹³ A ball and stick diagram of this complex has been shown in Figure 1.

Crystal Structure of Complex 2. The coordination environment of the Mn(II) ion, with atom numbering scheme, is shown in Figure 2. The Mn(II) ion displays octahedral coordination environment with the two chelated oxygen atoms (O1, O3) and two bridging oxygen atoms (O2, O4) of three different malonate ligands in the equatorial plane, while one nitrogen atom (N1) of the 4,4'-bipy ligand and the oxygen atom (O5w) from the water molecule occupy the axial positions. Each malonate ligand is coordinated to three metal atoms via the four oxygen atoms, and these carboxylato-bridged Mn(II) centers assemble into square-grid-like $[\text{Mn}(\text{malonate})]_n$ corrugated sheets with grid dimensions of $5.561 \times 5.410\ \text{\AA}$ in the *ac*-plane as shown Figure 3. It is noteworthy that the layer topology of complex **2** differs from that found in the structure of **1**, $\text{Mn}(\text{malonate})\cdot(\text{H}_2\text{O})_2$.¹³ In the former all the metals are coplanar, while in complex **2** the equatorial plane of malonate oxygens with manganese is organized in a stair-like fashion (Figure 4). The μ -4,4'-bipy ligands link the neighboring $[\text{Mn}(\text{malonate})]_n$ sheets to generate an infinite three-dimensional coordination

(21) North, A. C. T.; Philips, D. C.; Mathews, F. S. *Acta Crystallogr.* **1986**, *A24*, 351.

(22) Wilson, A. J. C. *International Tables for X-ray Crystallography*; Kluwer: Dordrecht, The Netherlands, 1992; Vol. C, Tables 4.2.6.8 and 6.1.1.4.

(23) Sheldrick, G. M. *SHELXS 97, Program for the Solution of Crystal Structure*; University of Gottingen: Gottingen, Germany, 1997.

(24) Sheldrick, G. M. *SHELXL 97, Program for the Solution of Crystal Structure*; University of Gottingen: Gottingen, Germany, 1997.

(25) Farrugia, L. J. ORTEP-3 for Windows. *J. Appl. Crystallogr.* **1997**, *30*, 565.

(26) Spek, A. L. *PLATON, Molecular Geometry Program*; University of Utrecht: Utrecht, The Netherlands, 1999.

(27) Nakamoto, K. *Infrared Spectra of Inorganic and Coordination Compounds*, 4th ed; John Wiley & Sons: New York, 1986.

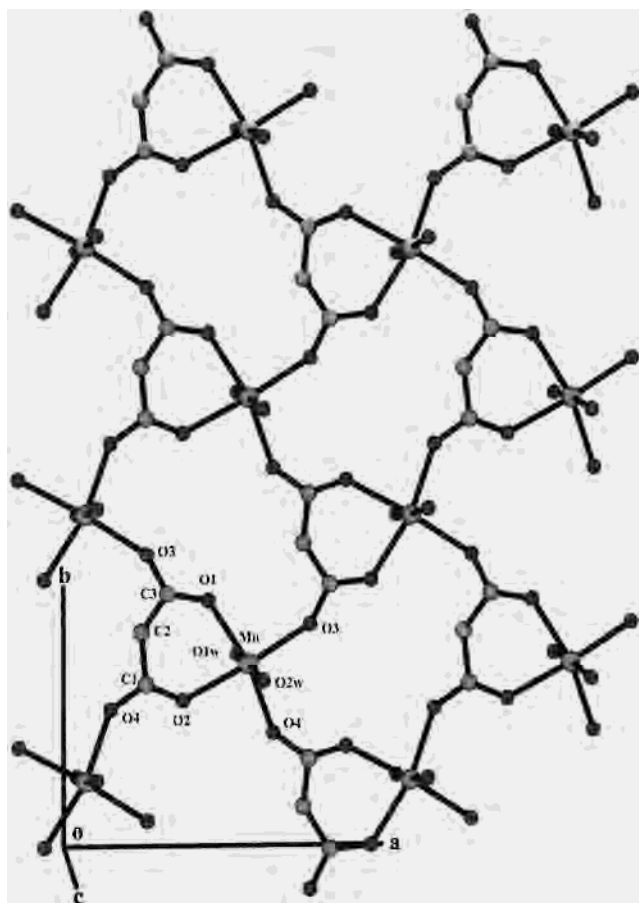


Figure 1. Ball and stick diagram of complex **1** showing the sheet-like structure in the *ab*-plane.

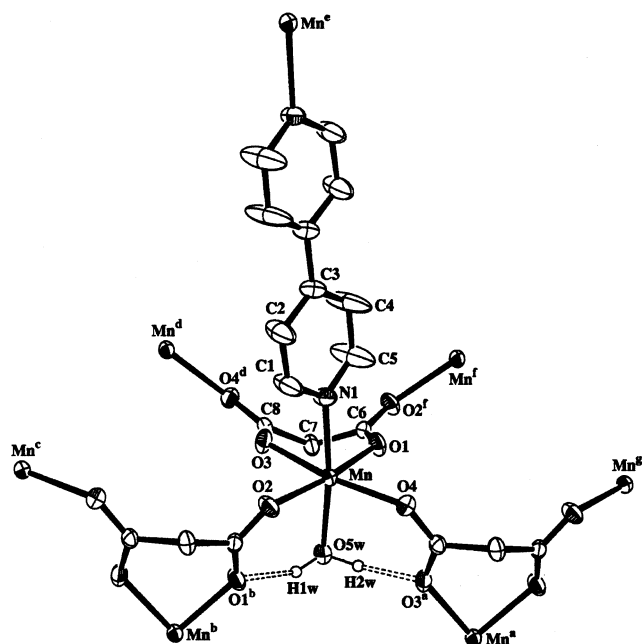


Figure 2. Local coordination environment of Mn(II) ion in the coordination polymer $[\text{Mn}(\text{malonate})(4,4'\text{-bipy})(\text{H}_2\text{O})]_n$. Atoms are drawn at 30% thermal ellipsoids. Dotted lines indicate H-bonds among the water molecules and adjacent oxygen atoms.

network with 6.1×4.4 Å channels parallel to the *a* direction (Figure 5). A similar network was found in the Co(II) analogue, $[\text{Co}_2(\text{mal})_2(\mu\text{-}4,4'\text{-bipy})(\text{H}_2\text{O})_2]_n$.¹²

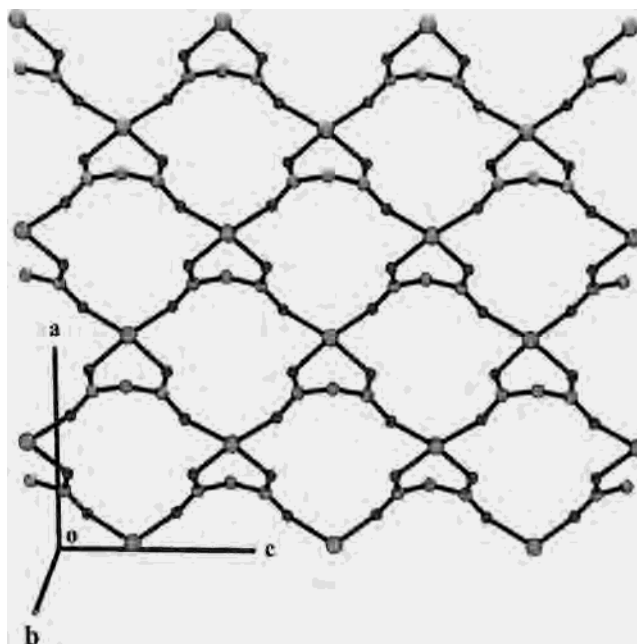


Figure 3. Square grid-like projection of Mn(malonate) layer of complex **2** lying in the *ac*-plane.

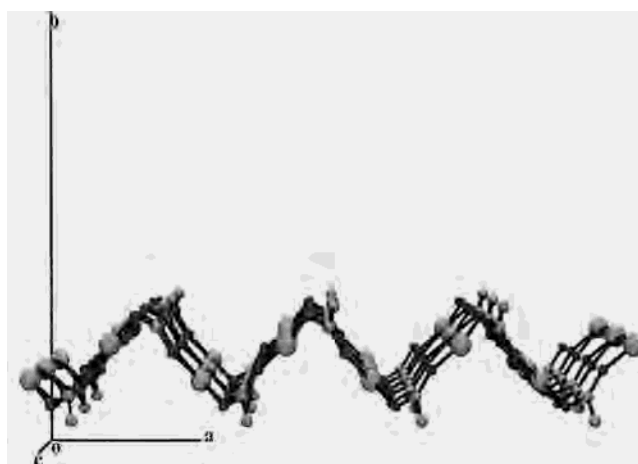


Figure 4. View of a Mn(malonate) layer of complex **2** showing a staircase-like arrangement of Mn atoms. (In complex **1** all Mn atoms are strictly planar.)

The Mn–O distances [Mn–O1 2.124(2) Å; Mn–O2 2.115(2) Å; Mn–O3 2.216(3) Å; Mn–O4 2.214(2) Å] associated with the chelating/bridging malonate ligands are similar to those of $[\text{Mn}(\text{malonate})(\text{H}_2\text{O})_2]$. The axial Mn–O(water) distance [Mn–O5w 2.236(3) Å] is larger than those found in complex **1**, and Mn–N distance [Mn–N1 2.290(3) Å] is within the range of those found in related octahedral Mn– $\mu\text{-}4,4'$ -bipy coordination polymers (2.276–2.336 Å).^{28–30} The Mn–Mn distances through Mn– $\mu\text{-}(O3\text{-}C8\text{-}O4)$ –Mn, Mn– $\mu\text{-}(O1\text{-}C6\text{-}O2)$ –Mn, and Mn– $\mu\text{-}4,4'$ -bipy–Mn bridges are 5.561, 5.410, and 11.723 Å, respectively. The coordinated

(28) Sain, S.; Maji, T. K.; Zangrando, E.; Ray Cahudhuri, N. *Transition Met. Chem.* **2002**, *27*, 000.

(29) Eppley, H. J.; de Vries, N.; Wang, S.; Aubin, S. M.; Tsai, H. L.; Foltig, K.; Hendrickson, D. N.; Christou, G. *Inorg. Chim. Acta* **1997**, *263*, 323.

(30) Li, M.-X.; Xie, G.-Y.; Gu, Y.-D.; Chen, J.; Zheng, P.-J. *Polyhedron* **1995**, *14*, 1235.

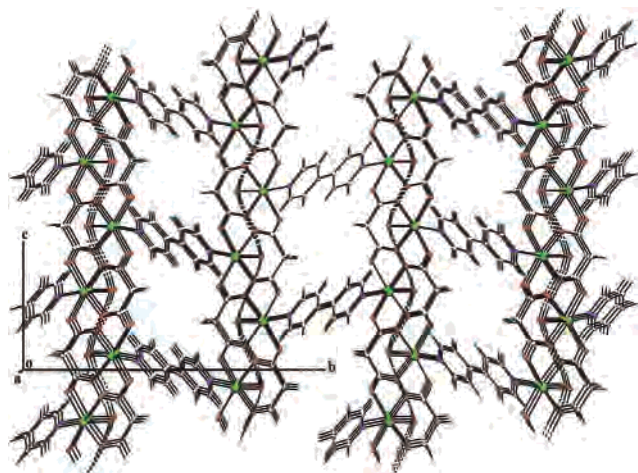
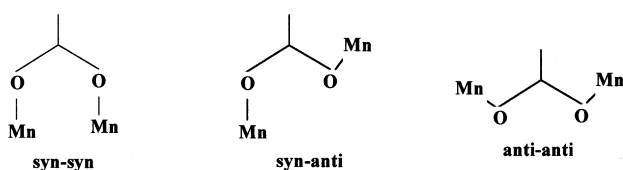


Figure 5. Molecular packing diagram of complex **2** showing channels formed between the Mn(malonate) layer and 4,4'-bipy ligands. [Color code: manganese, forest green; carbon, sky blue; hydrogen, yellow; nitrogen, deep blue; oxygen, red.]

Chart 1



water molecule forms intralayer hydrogen bonds to the O1 and O3 atoms [O1...O5w 2.673(4) Å; O3...O5w 2.745(4) Å].

Magnetic Properties. (A) Comments about the Exchange Coupling Generated by the Malonate (Carboxylato) Bridging Ligand. The carboxylato group is one of the most widely used bridging ligands for designing polynuclear complexes with interesting magnetic properties. Its versatility as a ligand is illustrated by the variety of its coordination modes while acting as a bridge,^{3a} the most common being the so-called *syn-syn*, *syn-anti*, and *anti-anti* modes (Chart 1). In general for any metal ion, the exchange coupling through the carboxylato moiety is highly dependent on the conformation of the bridge between the metal centers that are interacting.^{3b}

(a) *syn-syn* Carboxylato Bridge. A *syn-syn* pattern provides small metal–metal distances and results in a good overlap of the magnetic orbitals. This kind of coordination is usual in Mn(II) polynuclear complexes. It induces antiferromagnetic coupling, but in some cases, weak ferromagnetic coupling has been reported.^{5c} This kind of coordination is not present in our complexes.

(b) *syn-anti* Carboxylato Bridge. The *syn-anti* bridge for carboxylate ligands appears to be a rather uncommon binding mode for Mn(II) complexes.^{5d} A little is known about the magnetic properties of such carboxylato *syn-anti* manganese complexes. *syn-anti* carboxylato bridges induce very small J values because of the expanded metallic core and a mismatch in the orientation of magnetic orbitals.^{5d} The magnetic properties for *syn-anti* Mn(II) carboxylato-bridged complexes have been studied for a two-dimensional polymer,^{5e} [Mn^{II}(MCPA)₂(H₂O)₂]_n (MCPA = 2-methyl-4-chlorophen-

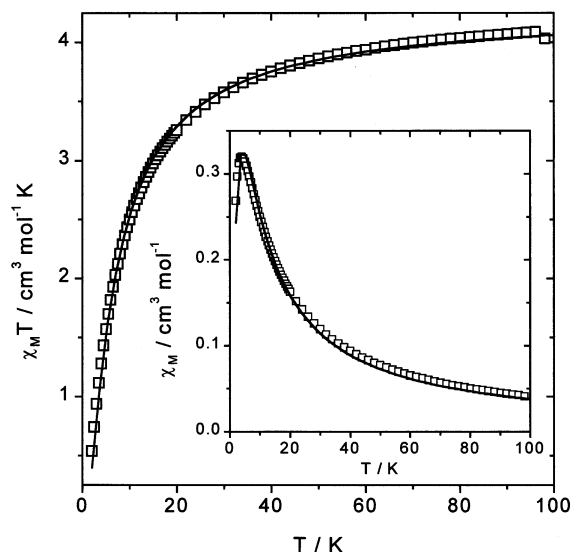


Figure 6. Plots of the temperature dependence (from 100 to 2 K) of χ_M (insert) and $\chi_M T$ for **1**. Solid lines (in χ_M and $\chi_M T$) represent the best theoretical fit (see text for the model and parameters).

oxyacetic acid), a one-dimensional polymer, [Mn(μ -3-ClPhCOO)₂(2,2'-bipy)₂]_n· n H₂O,^{5f} with two *syn-anti* carboxylato bridges, and discrete Mn(II) homodinuclear complexes involving either only one *syn-anti* carboxylato bridge, [Mn₂(2,2'-bipy)₂(H₂O)₂(Me₂NCH₂COO)](ClO₄),^{5g} or two *syn-anti* carboxylato bridges, [Mn₂(μ -PhCOO)₂(2,2'-bipy)₄](ClO₄)₂.^{5f} The antiferromagnetic coupling is always very small. When there are two carboxylato bridges,^{5f} the coupling parameter J is slightly greater than for only one carboxylato bridge.^{5f,g} All these exchange coupling constants are of the same order (between -0.2 and -2 cm⁻¹).

(c) *anti-anti* Carboxylato Bridge. This kind of coordination is less frequent than the other two for any metal. No complexes of Mn(II) have been reported so far with *anti-anti* conformation. For Cu(II) complexes, recent density functional theory (DFT) calculations,¹⁰ on a trinuclear copper(II) model with this *anti-anti* coordination mode, indicate that this coupling is antiferromagnetic.

Magnetic Properties of Complex 1. The temperature dependence of χ_M and $\chi_M T$ (χ_M being the magnetic susceptibility for one Mn^{II} ion) for complex **1** is shown in Figure 6 (from 100 to 2 K). The χ_M value is 0.00142 cm³ mol⁻¹ at 300 K. With decrease of the temperature, the values of the χ_M curve increase: from room temperature to 100 K (0.041 cm³ mol⁻¹) there is a smooth increase and from 100 to 2 K the increase is more pronounced reaching a maximum at 4 K ($\chi_M = 0.3197$ cm³ mol⁻¹). From 4 K there is a clear decrease of the χ_M (Figure 6, insert). $\chi_M T$ at 300 K is 4.25 cm³ mol⁻¹ K, a value which is as expected for an “isolated” Mn(II) ion. $\chi_M T$ is almost invariable up to 100 K (4.10 cm³ mol⁻¹ K) and gradually decreases when cooling to reach 0.538 cm³ mol⁻¹ K at 2.00 K. The shape of these curves is characteristic of the occurrence of weak antiferromagnetic interactions between the Mn(II) center.

Taking into account the two-dimensional character of **1**, the susceptibility data were fitted by following two approaches:

(a) The first was by the expansion series³¹ of Lines for an $S = 5/2$ antiferromagnetic quadratic layer, based on the exchange Hamiltonian $H = -\sum_{mn} J S_i S_j$, where \sum_{mn} runs over all pairs of nearest-neighbor spins i and j , eq 1, in which $\Theta = kT/|J|S(S + 1)$, $C_1 = 4$, $C_2 = 1.448$, $C_3 = 0.228$, $C_4 = 0.262$, $C_5 = 0.119$, $C_6 = 0.017$, and N , g , and β have their usual meanings.

$$Ng^2\beta^2/\chi|J| = 3\Theta + (\sum C_n/\Theta^{n-1}) \quad (1)$$

The best fit is given by the superexchange parameters $J = -0.36 \text{ cm}^{-1}$ and $g = 2.00$. In this assumption it has been assumed the quadratic character of the layer, i.e. only one J value. In fact, in complex **1** there are two J values, because there are two chemical pathways: *syn-anti* and *anti-anti* (Figure 1). As indicated above, both cases give weak antiferromagnetic coupling, which we can assume similar for the fit.

(b) The second was by means of the analytical expression derived by Curély for an infinite 2D square lattice composed of classical spins ($S = 5/2$) isotropically coupled and based on the exchange Hamiltonian $H = -\sum_{mn} J S_i S_j$, where S_{mn} runs over all pairs of nearest-neighbor spins i and j (Heisenberg couplings):³²

$$\chi = [Ng^2\beta^2S(S + 1)(1 + u^2)]/[3kT(1 - u^2)] \quad S = 5/2 \quad (2)$$

Here N is Avogadro's number, β Bohr's magneton, k Boltzmann's constant, and u the well-known Langevin function:

$$u = L(JS(S + 1)/kT) = \coth(JS(S + 1)/kT) - kT/JS(S + 1) \quad S = 5/2 \quad (3)$$

The best fit leads to $J = -0.32 \pm 0.002 \text{ cm}^{-1}$ and $g = 2.00 \pm 0.001$ (Figure 6). The agreement factor $R = \sum(\chi_{\text{m}}T_{\text{obs}} - \chi_{\text{m}}T_{\text{calc}})^2/\sum(\chi_{\text{m}}T_{\text{calc}})^2$ is 1.46×10^{-4} , which actually corresponds to an excellent experiment–theory agreement.

The J values obtained by Lines or Curély expressions are very similar: -0.36 and -0.32 cm^{-1} , respectively. Taking into account that the Curély formula is more accurate and is valid until 0 K (the Lines formula is only valid until the maximum of χ_{M} , approximately), the value of -0.32 cm^{-1} seems to be the most exact for complex **1**.

As indicated in the reported structural description, compound **1**¹³ is made up by a two-dimensional linkage of octahedral Mn(II) ions through malonate bridging ligands. The oxygen atoms (O1–O4) of three malonates (one of them chelated) are in the equatorial plane and O5w and O6w of water occupy the trans-axial positions. The pathways are shown in Figure 1. Two of the links are through Mn–O1–C1–O2–Mn (in *anti-anti* conformation) and the other two through Mn–O3–C2–O4–Mn (in *syn-anti* conformation). Both conformations create weak antiferromagnetic coupling.

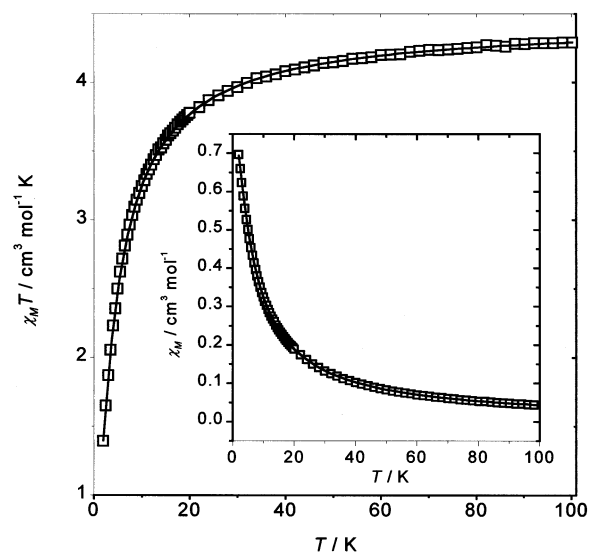


Figure 7. Plots of the temperature dependence (from 100 to 2 K) of χ_{M} (insert) and $\chi_{\text{M}}T$ for **2**. Solid lines (in χ_{M} and $\chi_{\text{M}}T$) represent the best theoretical fit (see text for the model and parameters).

Finally, there is a magnetic pathway Mn–O3–C2–C3–C1–O2–Mn, and this pathway through the three carbon atoms of the malonato-bridging ligand could be considered negligible.

Magnetic Properties of Complex 2. The temperature dependence of χ_{M} and $\chi_{\text{M}}T$ (χ_{M} being the magnetic susceptibility for one Mn(II) ion) for complex **2** is shown in Figure 7 (from 100 to 2 K), and the χ_{M} value is $0.00145 \text{ cm}^3 \text{ mol}^{-1}$ at 300 K. With decrease of the temperature, the values of χ_{M} increase; from room temperature to 100 K ($0.0428 \text{ cm}^3 \text{ mol}^{-1}$), there is a smooth increase, and from 100 to 2 K, the increase is more pronounced ($\chi_{\text{M}} = 0.6961 \text{ cm}^3 \text{ mol}^{-1}$ at 2 K). In this case there is no maximum in this χ_{M} curve. $\chi_{\text{M}}T$ at 300 K is $4.36 \text{ cm}^3 \text{ mol}^{-1} \text{ K}$, a value which is as expected for an “isolated” Mn(II) ion. $\chi_{\text{M}}T$ is almost invariable up to 100 K ($4.29 \text{ cm}^3 \text{ mol}^{-1} \text{ K}$) and gradually decreases when cooling to reach $1.39 \text{ cm}^3 \text{ mol}^{-1} \text{ K}$ at 2.00 K (Figure 7). The shape of these curves is characteristic of the occurrence of weak antiferromagnetic interactions between the Mn(II) center.

Taking into account that the structure is a three-dimensional network, it is impossible to fit the susceptibility data to find an appropriate J values. But the structure can be considered as two sublattices: a two-dimensional one, made by the Mn(II) ions linked by carboxylato bridging ligands (Figure 3), and these layers linked to each other by a 4,4'-bipy ligand (Figure 2). The bridging ligand 4,4'-bipy always gives a very small antiferromagnetic coupling.^{30,33,34} For $[\text{Mn}(\mu\text{-}4,4'\text{-bipy})(4,4'\text{-bipy})(\text{SCN})_2(\text{H}_2\text{O})_2]$, working only until 77 K, the corresponding authors state that “the magnetic behavior obeys a Curie law. There is practically no evidence of any magnetic exchange interaction between

(31) (a) Lines, M. E. *J. Phys. Chem. Solids* **1970**, *31*, 101. (b) Escuer, A.; Vicente, R.; Goher, M. A. S.; Mautner, F. A. *J. Chem. Soc., Dalton Trans.* **1997**, 4431 and references therein.

(32) (a) Curély, J. *Europhys. Lett.* **1995**, *32*, 529. (b) Curély, J. *Physica B* **1998**, *245*, 263. (c) Curély, J. *Physica B* **1998**, *254*, 277. (d) Curély, J.; Rouch, J. *Physica B* **1998**, *254*, 298.

(33) Rodríguez-Martín, Y.; Ruiz-Pérez, C.; Sanchiz, J.; Lloret, F.; Julve, M. *Inorg. Chim. Acta* **2001**, *318*, 159.

(34) Shen, H.-Y.; Liao, D.-Z.; Jiang, Z.-H.; Yan, S.-P.; Sun, B.-W.; Wang, G.-L.; Yao, X.-K.; Wang, H.-G. *Polyhedron* **1998**, *17*, 1953 and references therein.

the adjacent metal ions".³⁰ Very recently, Rodríguez-Martin et al. found a J value of -0.052 cm^{-1} through the 4,4'-bipy in $[\text{Cu}_2(\text{mal})_2(\text{H}_2\text{O})_2(4,4'\text{-bpy})]$.³³ It is interesting to consider this small J value, because this copper complex has, precisely, malonato and 4,4'-bipy, the same ligands that are in complex **2**.

Thus, the first hypothesis is considering complex **2** as a 2D magnetic lattice, assuming J (due to 4,4'-bipy) as zero. Then, the susceptibility data were fitted by the expansion series of Lines³¹ or Curély³² for an $S = 5/2$ antiferromagnetic quadratic layer, as made for complex **1**. The best fit is given by the superexchange parameters $J = -0.19 \pm \text{cm}^{-1}$ and $g = 2.00$ with $R = 2.35 \times 10^{-4}$ for the Lines expression and $J = -0.17 \text{ cm}^{-1}$ and $g = 2.00$ with $R = 1.10 \times 10^{-4}$ for the Curély expression.

As shown in Figure 2, two of the links are through Mn–O3–C8–O4–Mn (in *syn-anti* conformation) and the other two through Mn–O1–C6–O2–Mn (in *syn-anti* conformation). Both conformations create weak antiferromagnetic coupling. Finally, there is the pathway Mn–O4–C8–C7–C6–O2–Mn. As indicated above for **1**, this pathway through the three carbon atoms of the malonato-bridging ligand is slightly antiferromagnetic but not nil.

The second assumption is to make the fit through the molecular field approximation, assuming that there is a J' value between the planes much more smaller than the J value within the planes. For this, we can take the general formula given by Kahn,^{3b} introducing the zJ' value in the two formulas given above (Lines and Curély). With this assumption, using the Lines formula we did not find any good fit, but with the Curély formula we find the following values: J (in-plane) = -0.14 cm^{-1} , $J' = -0.031 \text{ cm}^{-1}$, and $g = 2.00$. R was excellent: 3.0×10^{-5} . Even if this fit is mathematically excellent, it must be taken with caution, because the main J value is too small and J' is not so different (very small). The molecular field model only is appropriate when the J'/J ratio is very small. Maybe the only conclusion we can state is that the interaction through 4,4'-bipy ligand (between the planes) is very weak in agreement with the large Mn–Mn separation (more than 11 Å) but it is not negligible. The same conclusion is given by Rodríguez-Martín et al. for an analogous copper complex.³³ We can conclude this study of the magnetic properties by corroborating that the malonato-bridging ligand has the ability to mediate weak antiferromagnetic interaction through the carboxylato bridge in *syn-anti* and *anti-anti* conformations (**1** and **2**).

EPR Measurement. The EPR spectrum of complex **1** measured on a polycrystalline powder at room temperature shows an isotropic signal centered at $g = 2.00$, line width 180 G (Figure 8). The spectra measured at variable temperature are practically identical, but the line width of the signal increases (at 4 K is 450 G) (Figure 8). For the complex **2** the behavior is practically the same: an isotropic signal centered at $g = 2.00$, line width 180 G (Figure 8). The spectra measured at variable temperature are practically identical, but the line width of the signal increases (at 4 K is 380 G) (Figure 8). If the EPR signal vanishes at low temperature,

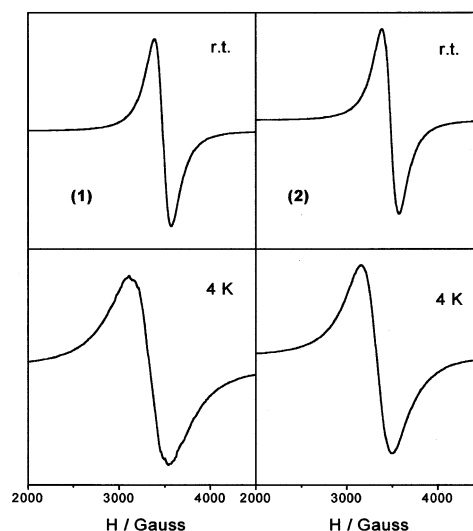


Figure 8. X-band EPR spectra for complexes **1** and **2** at room temperature and 4 K, showing broadening of the signal at low-temperature.

this would indicate antiferromagnetic ordering below the temperature of the transition.^{5e,31b,35} In the present case the EPR signal does not vanish at 4 K (only becomes broader) indicating that the possible magnetic ordering needs lower temperature (lower than 2 K, as shown for the χ_M values) (see above). This feature is consistent with the fact that the coupling constant created either by *syn-anti* carboxylate or 4,4'-bipy is always small. It is interesting to point out that complexes **1** and **2** show the same behavior, although the complex **1** is a 2D net and complex **2** is a 3D network. In fact, for complex **1**, the minimum Mn–Mn distances between each layer is 5.58 and 5.40 Å (in a layer is 5.807 Å), the minimum O–O distances between layers is 3.30 Å, and the minimum hydrogen bond distances between layers is 2.803 Å. For the complex **2**, the distances between Mn–Mn of two different layers is 11.723 Å. Thus, the presence of the 4,4'-bipy bridging ligand, which creates weak antiferromagnetic coupling, separates the layers and balances the dipolar and hydrogen-bond interactions present in the 2D system (complex **1**). The final effect is practically the same.

Thermal Investigations. The thermogravimetric analyses of compounds **1** and **2** show occurrence of three consecutive processes, namely dehydration, ligand pyrolysis, and inorganic residue formation. The TGA analysis for complex **1** shows the loss of two water molecules at ca. $\sim 200 \text{ }^\circ\text{C}$, corroborating the presence of strong H-bonding interactions for the $\text{O}(\text{malonate})\cdots\text{H}-\text{O}-\text{H}$ moiety. The dehydrated compound remains stable up to $\sim 280 \text{ }^\circ\text{C}$ without any weight loss, and at temperature range 280–320 $^\circ\text{C}$ the pyrolysis of the malonate ligand occurs resulting in the formation of MnO_2 as residue. The most interesting feature of complex **1** is that the dehydrated compound is stable in humid (RH $\sim 60\%$) atmosphere.

The TGA analysis of complex **2** reveals that each water molecule attached to the Mn(II) center is lost at $\sim 150 \text{ }^\circ\text{C}$. This suggests that water molecules are in strong H-bonding

(35) Goher, M. A. S.; Morsy, M. A. M.; Mautner, F. A.; Vicente, R.; Escuer, A. *Eur. J. Inorg. Chem.* **2000**, 1819.

interactions and the dehydrated compound gets rehydrated on exposure to humid (RH \sim 60%) atmosphere. The dehydrated compound remains stable up to \sim 330 °C, and upon further heating it loses initially 4,4'-bipyridine. As the temperature increases simultaneous 4,4'-bipyridine and malonate ligand pyrolyses occur with the occurrence of endothermic and exothermic peaks overlapping with each other resulting in the formation of MnO₂.

Conclusions

The magnetic properties of the complexes **1** and **2** may be compared with those of other two-dimensional manganese(II) systems that show weak antiferromagnetic coupling and for which magnetic ordering is not yet achieved at the lowest limit of the measurement temperature. For $[\{\text{Mn}(\text{SCN})_2(\text{EtOH})_2\}_2]^{31\text{b}}$ the superexchange parameter J takes the value of -1.22 cm^{-1} and the low-temperature EPR spectra show an increase in the line width at low temperature, but the susceptibility plot does not show important deviations from the theoretical two-dimensional susceptibility plot even at low temperature. For $[\{\text{Mn}(\text{minc})_2(\text{N}_3)_2\}_n]^{31\text{b}}$ ($J = -2.24 \text{ cm}^{-1}$) the low-temperature susceptibility plot deviates from the ideal two-dimensional behavior but does not achieve

magnetic ordering properties (at least down to 2 K). This is consistent with the relation between the critical temperature and J (greater J gives greater T_c). Other complexes of the family of the azido $[\{\text{MnL}_2(\text{N}_3)_2\}_n]$ systems offer properties similar to those of the M_2MnF_4 ($\text{M} = \text{Rb}, \text{K}$) systems^{31a} (high J values) and an important increase in T_c , in contrast with compounds with carboxylato bridges (as complexes **1** and **2**) which, in all reported cases, allow weak antiferromagnetic coupling.

Acknowledgment. Funding for the work described here is provided by the Council of Scientific and Industrial Research (New Delhi) Grants Scheme (granted to N.R.C.) and is gratefully acknowledged. J.R. and M.M. acknowledge the financial support given by the Spanish Government (Grant BQU2000-0791).

Supporting Information Available: X-ray crystallographic data, in CIF format, and tables giving crystal data and details of the structure determination, bond lengths and angles, atomic and hydrogen coordinates, equivalent displacement parameters, and anisotropic parameters. This material is available free of charge via the Internet at <http://pubs.acs.org>.

IC020238J